

**Report on the Scientific Validation  
of the mini-map photometry processing in the  
PHT pipeline**

**Phil Richards**  
(UK ISO Data Centre, CCLRC, RAL)

and

**Ulrich Klaas**  
(ISOPHOT Data Centre at MPIA)

Version 1.0

August 20, 2002

Rutherford Appleton Laboratory, Chilton, UK

# Contents

<b>1</b>	<b>Introduction</b>	<b>4</b>
<b>2</b>	<b>Caveats</b>	<b>4</b>
2.1	Photometry only applies to point sources . . . . .	4
2.2	Raster patterns processed . . . . .	4
<b>3</b>	<b>The pipeline algorithm</b>	<b>4</b>
<b>4</b>	<b>Comparison of Test Cases</b>	<b>6</b>
4.1	Point Source Photometry from PHT22 Mini-Maps: The SED of HR 7980 . . .	7
4.1.1	Motivation . . . . .	7
4.1.2	Method . . . . .	7
4.1.3	Results . . . . .	7
4.1.4	Conclusions . . . . .	7
4.1.5	Evaluation Log . . . . .	9
4.2	Point Source Photometry from PHT22 Mini-Maps: The SED of HR 1654 . . .	10
4.2.1	Motivation . . . . .	10
4.2.2	Method . . . . .	10
4.2.3	Results . . . . .	10
4.2.4	Conclusions . . . . .	10
4.2.5	Evaluation Log . . . . .	12
4.3	Point Source Photometry from PHT22 Mini-Maps: The SED of HR 7310 . . .	13
4.3.1	Motivation . . . . .	13
4.3.2	Method . . . . .	13
4.3.3	Results . . . . .	13
4.3.4	Conclusions . . . . .	13
4.3.5	Evaluation Log . . . . .	15
4.4	Point Source Photometry from PHT22 Mini-Maps: The SED of Sirius (HR 2491)	16
4.4.1	Motivation . . . . .	16
4.4.2	Method . . . . .	16
4.4.3	Results . . . . .	16
4.4.4	Conclusions . . . . .	16
4.4.5	Evaluation Log . . . . .	18
4.5	Point Source Photometry from PHT22 Mini-Maps: The 180 $\mu\text{m}$ flux of $\alpha$ Ari (HR 617) . . . . .	19
4.5.1	Motivation . . . . .	19
4.5.2	Method . . . . .	19
4.5.3	Results . . . . .	19
4.5.4	Conclusions . . . . .	19
4.5.5	Evaluation Log . . . . .	21
4.6	Point Source Photometry from PHT22 Mini-Maps: The 90 $\mu\text{m}$ flux of HR 6464	22
4.6.1	Motivation . . . . .	22
4.6.2	Method . . . . .	22
4.6.3	Results . . . . .	22
4.6.4	Conclusions . . . . .	22
4.6.5	Evaluation Log . . . . .	24
4.7	Point Source Photometry from PHT22 Mini-Maps: The 60 $\mu\text{m}$ flux of HD 185144	25
4.7.1	Motivation . . . . .	25
4.7.2	Method . . . . .	25
4.7.3	Results . . . . .	25
4.7.4	Conclusions . . . . .	25
4.7.5	Evaluation Log . . . . .	27
4.8	Point Source Photometry from PHT22 Mini-Maps: The FIR SED of Vega (HR 7001) . . . . .	28
4.8.1	Motivation . . . . .	28
4.8.2	Method . . . . .	28
4.8.3	Results . . . . .	28
4.8.4	Conclusions . . . . .	28

4.8.5	Evaluation Log . . . . .	30
4.9	Point Source Photometry from PHT22 Mini-Maps: The FIR SED of HD 216956 (Formalhaut) . . . . .	31
4.9.1	Motivation . . . . .	31
4.9.2	Method . . . . .	31
4.9.3	Results . . . . .	31
4.9.4	Conclusions . . . . .	31
4.9.5	Evaluation Log . . . . .	33
4.10	Point Source Photometry from PHT22 Mini-Maps: The SED of the Quasar PG 1700+518 . . . . .	34
4.10.1	Motivation . . . . .	34
4.10.2	Method . . . . .	34
4.10.3	Results . . . . .	34
4.10.4	Conclusions . . . . .	34
4.10.5	Evaluation Log . . . . .	36
<b>5</b>	<b>Summary and Conclusions</b>	<b>37</b>

# 1 Introduction

This report follows a similar format to the scientific validation of OLP V10. The same calibration files were used, so the photometry is expected to be identical. However, the algorithm used to derive the flux densities from the PCAS file has now been implemented in the pipeline code and the results from this algorithm are compared with the results from the IDL procedure which has been used for the validation of V9 [1] and V10 [3] OLP. The pipeline generates the surface brightnesses, which are written to the PCAS file, according to the algorithms described in the PHT Handbook [2].

At present the point-spread function correction factors are only available for intervals corresponding to the separation of adjacent pixels in the PHT-C arrays. Therefore only observations with an integral number of pixel offsets, that is raster steps of 46'' for the C100 array and raster steps of 92'' for the C200 array, have been reprocessed. Also only those test cases with these raster parameters have been validated, so the test cases examined do not correspond exactly to those used in the V10 validation.

The pipeline algorithm is described in detail in section 3. It is very similar to Kiss [1] algorithm, but there are minor differences. These differences are not significant, but the photometry from the PCASPHT method and the pipeline algorithm can differ by a few percent.

## 2 Caveats

### 2.1 Photometry only applies to point sources

This report demonstrates that for POINT sources, the flux densities derived by the pipeline processing are in very good agreement with IRAS and model flux densities. However, the processing algorithm in the pipeline assumes that a fit is being made to a point source. If the source is not a true point source, then the flux density in the PGAI product will underestimate the flux of the source. For example, for Vega, where there is an extended component due to the presence of a cool disk, the point source footprint gives a flux density, which is  $\sim 15\%$  lower than the flux from a footprint that takes into account the extended emission from the disk and gives a good fit to the model. Therefore care has to be taken if it is suspected that the source is extended.

### 2.2 Raster patterns processed

As the footprint fraction factors are only defined for the pixel separations of the C100 and C200 arrays, only observations with an integral number of pixel offsets, that is raster steps of 46'' for the C100 array and raster steps of 92'' for the C200 array, have been reprocessed. A summary of the observations processed per raster pattern is as follows:

C100

3x3 raster pattern: 471 observations  
other raster patterns: 35 observations

C200

2x2 raster pattern: 161 observations  
4x2 raster pattern: 132 observations  
other raster patterns: 50 observations

## 3 The pipeline algorithm

The pipeline algorithm is an implementation of the PCASPHT method developed by Kiss [1]. It is based on the determination of fluxes for each individual pixel alone. Each pixel at each raster position sees a certain amount of the flux from the central (point) source plus the

background, which is assumed to be constant at all positions:

$$F_{ij} = f_{ij} \times F_j^S + F_j^{BG}$$

Here  $F_j^S$  is the total flux (Jy/pixel) of the central source measured by the  $j$ th pixel,  $F_j^{BG}$  is the constant background flux, measured by the  $j$ th pixel,  $f_{ij}$  is the fraction of the central source flux on the  $j$ th pixel at the  $i$ th raster position and  $F_{ij}$  is the measured flux on the  $j$ th pixel at the  $i$ th raster position. The  $f_{ij}$ -s used in the processing have been established empirically by Laureijs (1999) [4]. The  $F_{ij}$ -s are the measured fluxes, so there are only two parameters to determine,  $F_j^S$  and  $F_j^{BG}$  for the  $j$ th pixel, which is done by a simple line-fit using the  $F_{ij}$ -s as a linear function of  $f_{ij}$ -s. The final source flux density and background flux are determined from the bi-weight mean of the values from all the pixels. The values for the  $f_{ij}$ -s are given below in Tables 1 and 2.

In the processing of raster maps by the pipeline, in order to co-add the surface brightness values onto the image grid, the position of each pixel is determined in image coordinates  $(x_{ij}, y_{ij})$  with the origin of the image at the centre of the raster. Thus the offset of pixel  $j$  at raster position  $i$  relative to the centre of the source (assumed to be at the centre of the raster),  $r_{ij}$ , is:

$$r_{ij} = \sqrt{x_{ij}^2 + y_{ij}^2}$$

The footprint fraction factor  $f(r_{ij})$  corresponding to the offset  $r_{ij}$  is assigned according to the following offset ranges://

For C100:

$$\begin{aligned} r_{ij} \leq 23.0 & \implies f(r_{ij}) = f(0) \\ 23.0 < r_{ij} \leq 55.5 & \implies f(r_{ij}) = f(46) \\ 55.5 < r_{ij} \leq 78.05 & \implies f(r_{ij}) = f(46)\sqrt{2} \\ 78.05 < r_{ij} \leq 115.0 & \implies f(r_{ij}) = f(92) \\ 115.0 < r_{ij} & \implies f(r_{ij}) = f(> 92) \end{aligned}$$

For C200:

$$\begin{aligned} r_{ij} \leq 46.0 & \implies f(r_{ij}) = f(0) \\ 46.0 < r_{ij} \leq 111.05 & \implies f(r_{ij}) = f(92) \\ 111.05 < r_{ij} \leq 157.0 & \implies f(r_{ij}) = f(92)\sqrt{2} \\ 157.0 < r_{ij} & \implies f(r_{ij}) = f(> 92) \end{aligned}$$

filter	Centre PSF	$f(0)$	$f(46)$	$f(46\sqrt{2})$	$f(92)$	$f(> 92)$
50 $\mu$ m	0.656	1.0	0.0465	0.0077	0.0019	0.0
60 $\mu$ m	0.667	1.0	0.0375	0.0057	0.0015	0.0
70 $\mu$ m	0.629	1.0	0.0632	0.0171	0.0025	0.0
90 $\mu$ m	0.586	1.0	0.0553	0.0187	0.0014	0.0
100 $\mu$ m	0.558	1.0	0.0598	0.0292	0.0020	0.0
105 $\mu$ m	0.540	1.0	0.0699	0.0336	0.0037	0.0

Table 1: The footprint fractions of the C100 detector array for each filter.  $f(0)$ ,  $f(46)$ ,  $f(46\sqrt{2})$  and  $f(92)$  denote the footprint fraction factors at a distance of 0, 46,  $46\sqrt{2}$  and 92'' from the center of the source (PSF), respectively.

The  $f_{ij}$ -s for filter  $k$  are then given by:

$$f_{ij} = f_{psf}(k)f(r_{ij})$$

where  $f_{psf}(k)$  is the central PSF factor for filter  $k$  given in column 2 of Tables 1 and 2. In addition to the bi-weight average over the pixels, the median values for the source flux density and background are also determined. For the C100 array, the pixels which give the

filter	Centre PSF	$f(0)$	$f(92)$	$f(92\sqrt{2})$	$f(> 92)$
120 $\mu\text{m}$	0.678	1.0	0.0589	0.0161	0.0
135 $\mu\text{m}$	0.641	1.0	0.0763	0.0266	0.0
160 $\mu\text{m}$	0.620	1.0	0.0656	0.0298	0.0
180 $\mu\text{m}$	0.609	1.0	0.0946	0.0371	0.0
200 $\mu\text{m}$	0.568	1.0	0.0989	0.0525	0.0

Table 2: The footprint fractions of the C200 detector array for each filter.  $f(0)$ ,  $f(92)$ ,  $f(92\sqrt{2})$  denote the footprint fraction factors at a distance of 0, 92 and  $92\sqrt{2}$  from the center of the source(PSF), respectively.

median source flux and background are saved in the header. The flux densities for the source and background for each filter,  $n$ , are stored in the following keywords in the PGAI product header:

```

SOURCE $n$  = Flux density (source)(Jy)
SOURCEUn = Uncertainty in flux (source)(Jy)
BACK $n$  = Measured background (MJy/sr)
BACKUn = Background uncertainty(MJy/sr)
BACKF $n$  = Measured background (Jy/pixel)
BACKFUn = Background uncertainty(Jy/pixel)
SRCMED $n$  = Median flux density (source)(Jy)
SRCMDUn = Unc. in median flux (source)(Jy)
SRCPIX $n$  = Pixel giving median flux (C100 only)
BSBMED $n$  = Median measured background (MJy/sr)
BSBMDUn = Median background uncertainty(MJy/sr)
BFMED $n$  = Median measured background (Jy/pixel)
BFMEDUn = Median background uncertainty(Jy/pixel)
BCKPIX $n$  = Pixel giving median background (C100 only)

```

The flux densities associated with the SOURCE $n$  and SRCMED $n$  keywords are POINT source flux densities, that is they are only correct if the source being mapped is a point source and there is no associated extended emission.

The SRCPIX $n$  keyword gives the pixel out of the 9 pixels in the C100 array (see PHT Handbook [2] for pixel numbering) which has the median flux density (SRCMED $n$  keyword) and the BCKPIX $n$  keyword gives the equivalent pixel for the median background.

## 4 Comparison of Test Cases

Note that the flux densities given in the plots and tables for comparison with OLP 10 are the bi-weight averages over all the pixels (given by the SOURCE $n$  keywords).

## 4.1 Point Source Photometry from PHT22 Mini-Maps: The SED of HR 7980

### 4.1.1 Motivation

For HR 7980 there exist mini-maps in all C100 filters and in three out of five C200 filters (120 to 170  $\mu\text{m}$ ). Therefore, the relative photometry from the different implementations can be checked for most of the filters.

### 4.1.2 Method

We compare the background subtracted, color corrected flux values of OLP V10 and OLP PHTRP001 results against the model prediction.

### 4.1.3 Results

The comparison of OLP 10 and OLP PHTRP001 photometry with the model is given in part 1 of the evaluation log. Fig. 1 displays the photometric results extracted from the mini-map PCAS product for V10 (top) and from the PGAI header for PHTRP001 (bottom). The C100 photometry is as accurate as 10% for all filters, except for the 105  $\mu\text{m}$  filter. But here the photometry is now improved on V10 and is now  $< 20\%$ . The C200 photometry is better than 20% for the 120 and 150  $\mu\text{m}$  filters. However, at 170  $\mu\text{m}$  the bi-weight mean flux differs by  $\sim 50\%$  from the model and  $\sim 30\%$  from the OLP 10 value, whereas the PHTRP001 median flux gives better agreement with OLP 10. It is not yet clear why there is such a large difference for this filter when, for most other filters, the PHTRP001 bi-weight mean flux densities give better agreement with the model compared to OLP V10. The IRAS 100  $\mu\text{m}$  FSC flux has only medium quality.

### 4.1.4 Conclusions

- This test case shows that there is very good agreement found between the OLP 10 photometry derived from the PCAS products and the PHTRP001 photometry derived from a similar algorithm for all C100 filters and for two out of five C200 filters.
- The C100 absolute photometric accuracy is  $< 20\%$ , for filters shortward of 100  $\mu\text{m}$  even  $< 10\%$ .
- The C200 absolute photometric accuracy is  $< 20\%$  for the 120 and 150  $\mu\text{m}$  filters.
- For the 170  $\mu\text{m}$  filter, the PHTRP001 bi-weight mean flux differs significantly from the median value and the model.

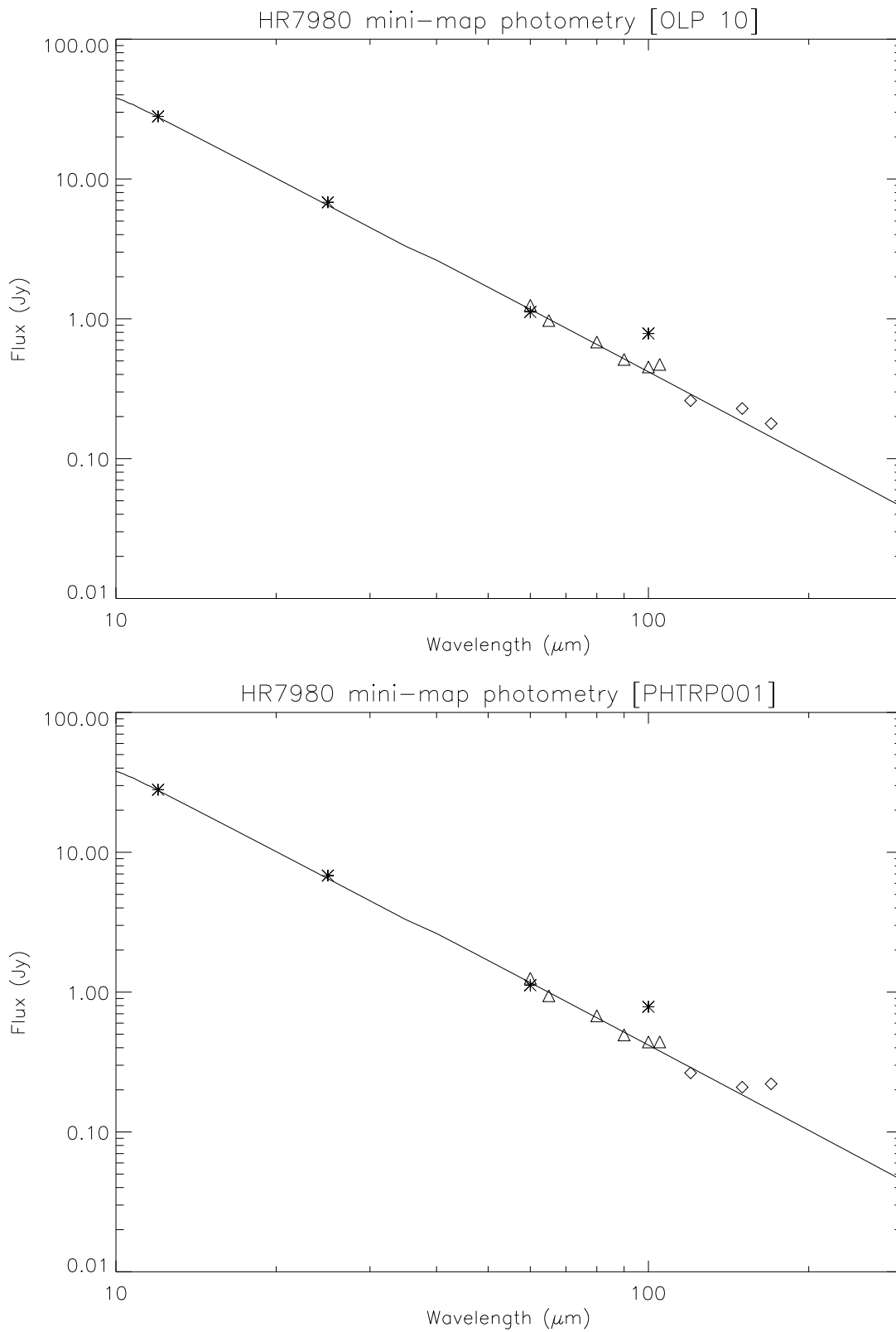


Figure 1: Comparison of PHT-C mini-map photometry with the model spectrum (plus extension out to  $300 \mu\text{m}$ ) of HR7980 provided by M. Cohen and with IRAS photometry for OLP 10 (upper panel) and OLP PHTRP001 (lower panel). All photometric points are color corrected for a 3850 K BB. The meaning of the symbols is the following: solid line: model, asterisk: IRAS, triangle: PHT-C100 (P22 AOT), diamond: PHT-C200 (P22 AOT).



### 4.1.5 Evaluation Log

1) point source photometry of HR7980 from mini-maps

Measurements:

PHT-C100:      pcas72701415 (P22 minimap)      FCS = 60 um  
                   pcas72701412 (P22 minimap)      FCS = 65 um  
                   pcas72701409 (P22 minimap)      FCS = 80 um  
                   pcas72701418 (P22 minimap)      FCS = 90 um  
                   pcas72701406 (P22 minimap)      FCS = 100 um  
                   pcas72701403 (P22 minimap)      FCS = 105 um  
 PHT-C200:      pcas73401709 (P22 minimap)      FCS = 120 um  
                   pcas73401603 (P22 minimap)      FCS = 150 um  
                   pcas73401706 (P22 minimap)      FCS = 170 um

Colour correction: black body, T = 3850K

Model:            Cohen

The PHTRP001 flux densities are those given by the SOURCEn keywords in the PGAI product headers for the above TDTs.

Det	cwl ( $\mu\text{m}$ )	OLP 10	PHTRP001	IRAS	Model	$\Delta$ (OLP 10)	$\Delta$ (PHTRP001)
C1	60.0	1.248	1.254	1.118	1.169	6.80	7.31
C1	65.0	0.973	0.942		0.995	-2.30	-5.40
C1	80.0	0.682	0.677		0.655	4.11	3.26
C1	90.0	0.512	0.494		0.517	-0.96	-4.36
C1	100.0	0.453	0.440	0.785	0.418	8.35	5.27
C1	105.0	0.472	0.440		0.379	24.68	16.27
C2	120.0	0.260	0.264		0.289	-10.10	-8.61
C2	150.0	0.228	0.209		0.184	24.01	13.51
C2	170.0	0.178	0.221		0.143	24.65	54.61

The following table gives a comparison between the bi-weight mean and median flux densities (in Jy from the SOURCEn and SRCMEDn keywords respectively) and the bi-weight mean and median backgrounds (in Jy/pixel from the BACKFn and BFMEDn keywords respectively). No colour corrections have been applied to the flux densities in the table.

Det	cwl ( $\mu\text{m}$ )	Source Flux(Jy)		Background(Jy/pixel)	
		Bi-weight	Median	Bi-weight	Median
C1	60.0	1.330	1.277	1.453	1.416
C1	65.0	1.215	1.172	1.458	1.380
C1	80.0	0.833	0.855	1.185	1.164
C1	90.0	0.574	0.570	0.964	0.967
C1	100.0	0.484	0.490	0.891	0.892
C1	105.0	0.462	0.461	0.888	0.871
C2	120.0	0.320	0.321	2.690	2.559
C2	150.0	0.230	0.232	2.872	2.823
C2	170.0	0.265	0.229	2.953	2.876

## 4.2 Point Source Photometry from PHT22 Mini-Maps: The SED of HR 1654

### 4.2.1 Motivation

Also for HR 1654 there exist mini-maps in all C100 filters and in three out of five C200 filters (120 to 170  $\mu\text{m}$ ). Therefore, the relative photometry from the different implementations can be checked for consistency and against the models for most of the filters.

### 4.2.2 Method

We compare the background subtracted, color corrected flux values of OLP V10.0 and OLP PHTRP001 results against the model prediction.

### 4.2.3 Results

The comparison of OLP 10 and OLP PHTRP001 photometry with the model is given in part 1 of the evaluation log. Fig. 2 displays the photometric results extracted from the mini-map PCAS product for V10 (top) and from the PGAI header for PHTRP001 (bottom). The C100 photometry is as accurate as 10 % for all filters, with the PHTRP001 data for the 60 and 65  $\mu\text{m}$  filters slightly further off the model, but the flux density in the 105  $\mu\text{m}$  filter is much closer to the model. The C200 photometry from OLP PHTRP001 is also closer to the model for all filters and in fact <5 % for the 120 and 150  $\mu\text{m}$  filters.

### 4.2.4 Conclusions

- This test case shows that the good absolute photometric accuracy found for the PCAS products holds also for the PGAI products for all C100 filters and for three out of five C200 filters.
- The C100 absolute photometric accuracy is < 10 %, for all filters, the OLP 10 data being closer to the model for filters below 100  $\mu\text{m}$  and the opposite being the case for 100  $\mu\text{m}$  and above.
- The C200 absolute photometric accuracy from the PHTRP001 processing is <12 % for all filters (<5 % for 120 and 150  $\mu\text{m}$ ).

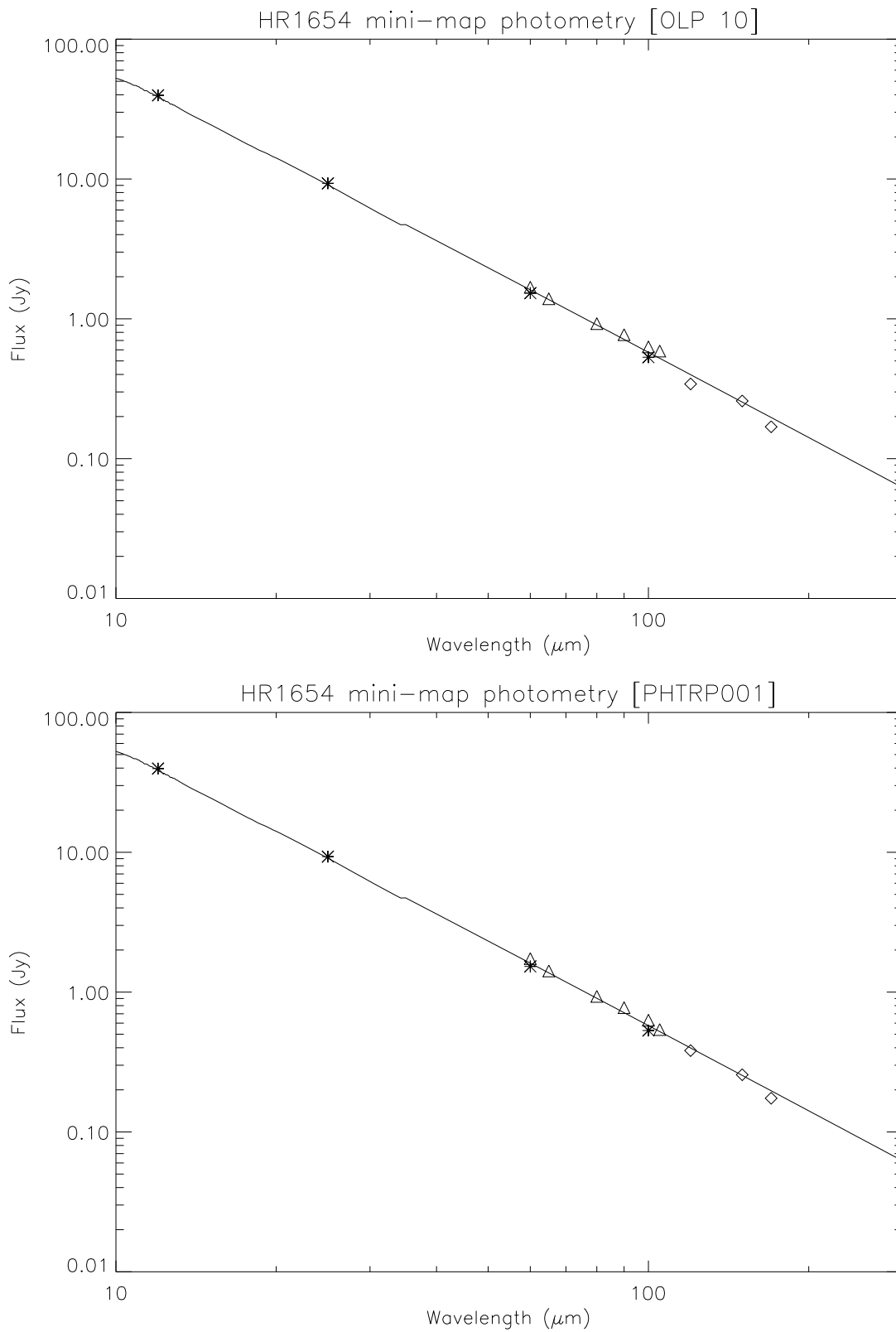


Figure 2: Comparison of PHT-C mini-map photometry with the model spectrum (plus extension out to  $300\ \mu\text{m}$ ) of HR1654 provided by M. Cohen and with IRAS photometry for OLP 10 (upper panel) and OLP PHTRP001 (lower panel). All photometric points are color corrected for a 4000 K BB. The meaning of the symbols is the following: solid line: model, asterisk: IRAS, triangle: PHT-C100 (P22 AOT), diamond: PHT-C200 (P22 AOT).

### 4.2.5 Evaluation Log

1) point source photometry of HR1654 from mini-maps

Measurements:

PHT-C100:      pcas65701315 (P22 minimap)      FCS = 60 um  
                   pcas65701312 (P22 minimap)      FCS = 65 um  
                   pcas65701309 (P22 minimap)      FCS = 80 um  
                   pcas65701318 (P22 minimap)      FCS = 90 um  
                   pcas65701306 (P22 minimap)      FCS = 100 um  
                   pcas65701303 (P22 minimap)      FCS = 105 um  
 PHT-C200:      pcas65002709 (P22 minimap)      FCS = 120 um  
                   pcas65002103 (P22 minimap)      FCS = 150 um  
                   pcas65002406 (P22 minimap)      FCS = 170 um

Colour correction: black body, T = 4000K

Model:            Cohen

The PHTRP001 flux densities are those given by the SOURCEn keywords in the PGAI product headers for the above TDTs.

Det	cwl ( $\mu\text{m}$ )	OLP 10	PHTRP001	IRAS	Model	$\Delta$ (OLP 10)	$\Delta$ (PHTRP001)
C1	60.0	1.682	1.736	1.527	1.610	4.47	7.82
C1	65.0	1.391	1.417		1.372	1.42	3.28
C1	80.0	0.924	0.932		0.903	2.24	3.18
C1	90.0	0.770	0.774		0.713	8.07	8.66
C1	100.0	0.630	0.629	0.531	0.576	9.38	9.22
C1	105.0	0.588	0.540		0.522	12.67	3.40
C2	120.0	0.342	0.382		0.399	-14.19	-4.26
C2	150.0	0.258	0.257		0.254	1.82	1.09
C2	170.0	0.169	0.174		0.197	-14.24	-11.61

The following table gives a comparison between the bi-weight mean and median flux densities (in Jy from the SOURCEn and SRCMEDn keywords respectively) and the bi-weight mean and median backgrounds (in Jy/pixel from the BACKFn and BFMEDn keywords respectively). No colour corrections have been applied to the flux densities in the table.

Det	cwl ( $\mu\text{m}$ )	Source Flux(Jy)		Background(Jy/pixel)	
		Bi-weight	Median	Bi-weight	Median
C1	60.0	1.840	1.841	0.557	0.539
C1	65.0	1.828	1.899	0.554	0.540
C1	80.0	1.146	1.139	0.486	0.473
C1	90.0	0.898	0.900	0.416	0.420
C1	100.0	0.692	0.692	0.371	0.359
C1	105.0	0.567	0.578	0.322	0.325
C2	120.0	0.462	0.435	1.174	1.114
C2	150.0	0.282	0.280	1.311	1.293
C2	170.0	0.209	0.210	1.339	1.309

## 4.3 Point Source Photometry from PHT22 Mini-Maps: The SED of HR 7310

### 4.3.1 Motivation

HR 7310 is a factor 5 – 6 fainter than the previous two stars HR 7980 and HR 1654. There exist mini-maps in the C100 100  $\mu\text{m}$  filter and in the same three out of five C200 filters (120 to 170  $\mu\text{m}$ ) as for the other two stars. Therefore, the relative photometry from the different implementations can be checked for a fainter source.

### 4.3.2 Method

We compare the background subtracted, color corrected flux values of OLP V10.0 and OLP PHTRP001 results against the model prediction.

### 4.3.3 Results

The comparison of OLP 10 and OLP PHTRP001 photometry with the model is given in part 1 of the evaluation log. Fig. 3 displays the photometric results extracted from the mini-map PCAS product. The C100 photometry is as accurate as 30 % for the 100  $\mu\text{m}$  filter. The IRAS 100  $\mu\text{m}$  FSC flux is only an upper limit. The C200 photometry is better than 25 % only for the 120  $\mu\text{m}$  filter. Expected source fluxes below 100 mJy which occur for this source at wavelengths longer than 120  $\mu\text{m}$  cannot be measured reliably any more.

### 4.3.4 Conclusions

- This test case shows some limits of this method for determining source photometry. Although, the flux densities are slightly closer to the model, the following conclusions, which applied to the OLP V10 data also apply to the PHTRP001 mini-map processing.
- At 100  $\mu\text{m}$  the photometric accuracy is better than 30 %.
- For C200 mini-map photometry a lower flux limit of 0.1 Jy is found below which photometry is not reliable any more.

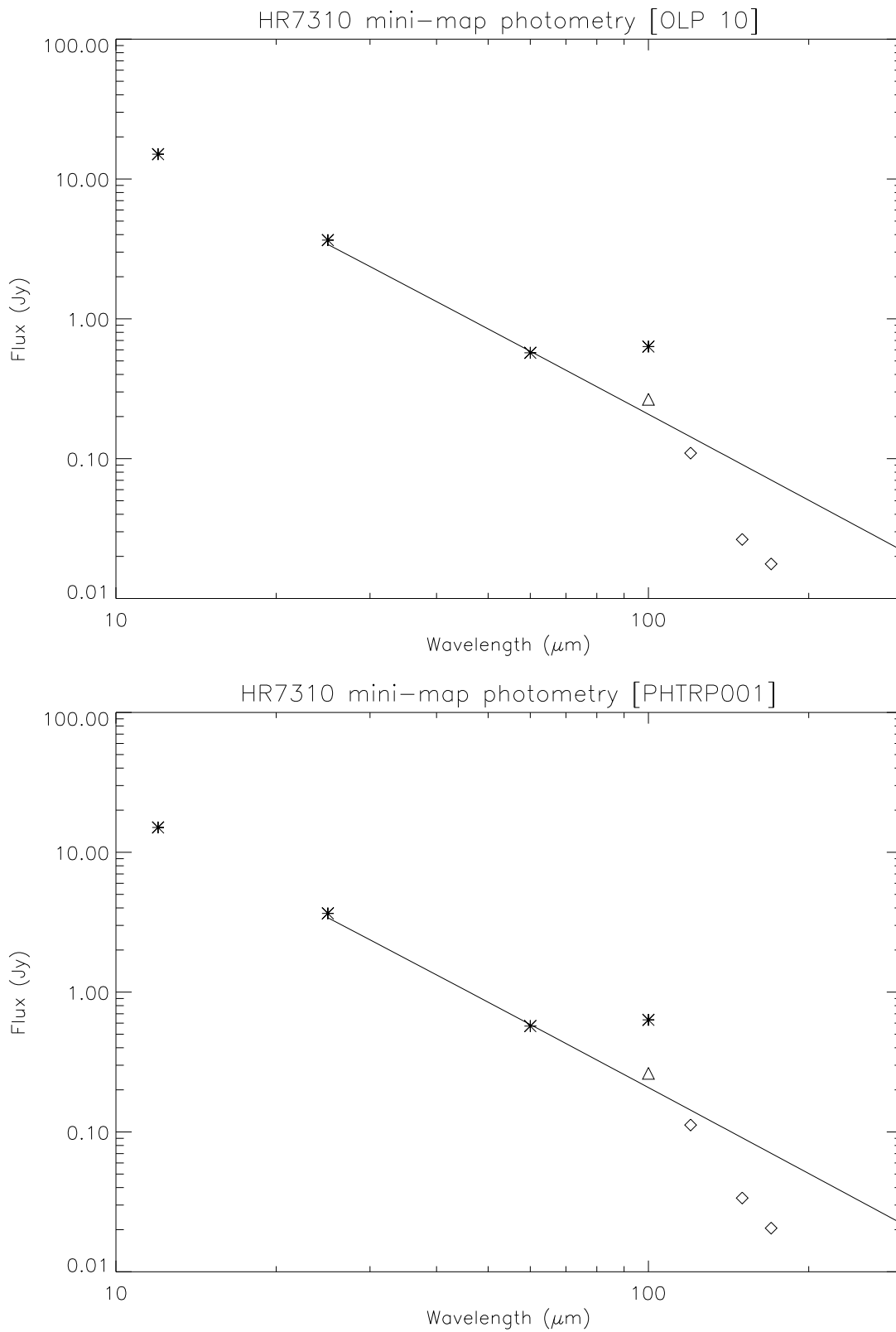


Figure 3: Comparison of PHT-C mini-map photometry with the model spectrum (plus extension out to  $300\ \mu\text{m}$ ) of HR 7310 provided by M. Cohen and with IRAS photometry for OLP 10 (upper panel) and OLP PHTRP001 (lower panel). All photometric points are color corrected for a 4852 K BB. The meaning of the symbols is the following: solid line: model, asterisk: IRAS, triangle: PHT-C100 (P22 AOT), diamond: PHT-C200 (P22 AOT).

### 4.3.5 Evaluation Log

1) point source photometry of HR 7310 from mini-maps

Measurements:

PHT-C100: pcas74800404 (P22 minimap) FCS = 100 um  
PHT-C200: pcas60100803 (P22 minimap) FCS = 120 um  
pcas60101009 (P22 minimap) FCS = 150 um  
pcas60100906 (P22 minimap) FCS = 170 um

Colour correction: black body, T = 4852K

Model: Cohen

The PHTRP001 flux densities are those given by the SOURCE<sub>n</sub> keywords in the PGAI product headers for the above TDTs.

Det	cwl ( $\mu\text{m}$ )	OLP 10	PHTRP001	IRAS	Model	$\Delta$ (OLP 10)	$\Delta$ (PHTRP001)
C1	100.0	0.266	0.262	0.634	0.208	27.92	26.36
C2	120.0	0.110	0.112		0.143	-23.47	-21.74
C2	150.0	0.026	0.034		0.091	-70.88	-62.90
C2	170.0	0.018	0.021		0.070	-74.88	-70.82

The following table gives a comparison between the bi-weight mean and median flux densities (in Jy from the SOURCE<sub>n</sub> and SRCMED<sub>n</sub> keywords respectively) and the bi-weight mean and median backgrounds (in Jy/pixel from the BACKF<sub>n</sub> and BFMED<sub>n</sub> keywords respectively). No colour corrections have been applied to the flux densities in the table.

Det	cwl ( $\mu\text{m}$ )	Source Flux(Jy)		Background(Jy/pixel)	
		Bi-weight	Median	Bi-weight	Median
C1	100.0	0.289	0.278	0.424	0.408
C2	120.0	0.136	0.138	1.358	1.351
C2	150.0	0.037	0.036	1.779	1.777
C2	170.0	0.025	0.026	1.591	1.557

## 4.4 Point Source Photometry from PHT22 Mini-Maps: The SED of Sirius (HR 2491)

### 4.4.1 Motivation

Sirius is one of the two primary calibrators. However, due to its limited visibility it was not used for establishment of the FCS calibration. Therefore, the C100 mini-map photometry of Sirius considered here provides an independent check of the measurement reproducibility.

### 4.4.2 Method

We compare the background subtracted, color corrected flux values of OLP V10 and OLP PHTRP001 results against the model prediction by Cohen and IRAS photometry.

### 4.4.3 Results

The comparison of OLP V10 and OLP PHTRP001 photometry with the model is given in part 1 of the evaluation log. Fig. 4 displays the photometric results extracted from the mini-map PCAS product for V10 (top) and the PGAI product header for PHTRP001 (bottom). The C100 photometry is as accurate as 15%. The IRAS 100  $\mu\text{m}$  PSC flux has only medium quality and shows a positive offset of 70%.

### 4.4.4 Conclusions

- This test case shows the good absolute photometric accuracy derived from the PCAS products ( $\sim 10\%$ ) has not been reproduced in the pipeline products for the 60  $\mu\text{m}$  filter. The pipeline flux densities at 60  $\mu\text{m}$  are 15% above the model flux.



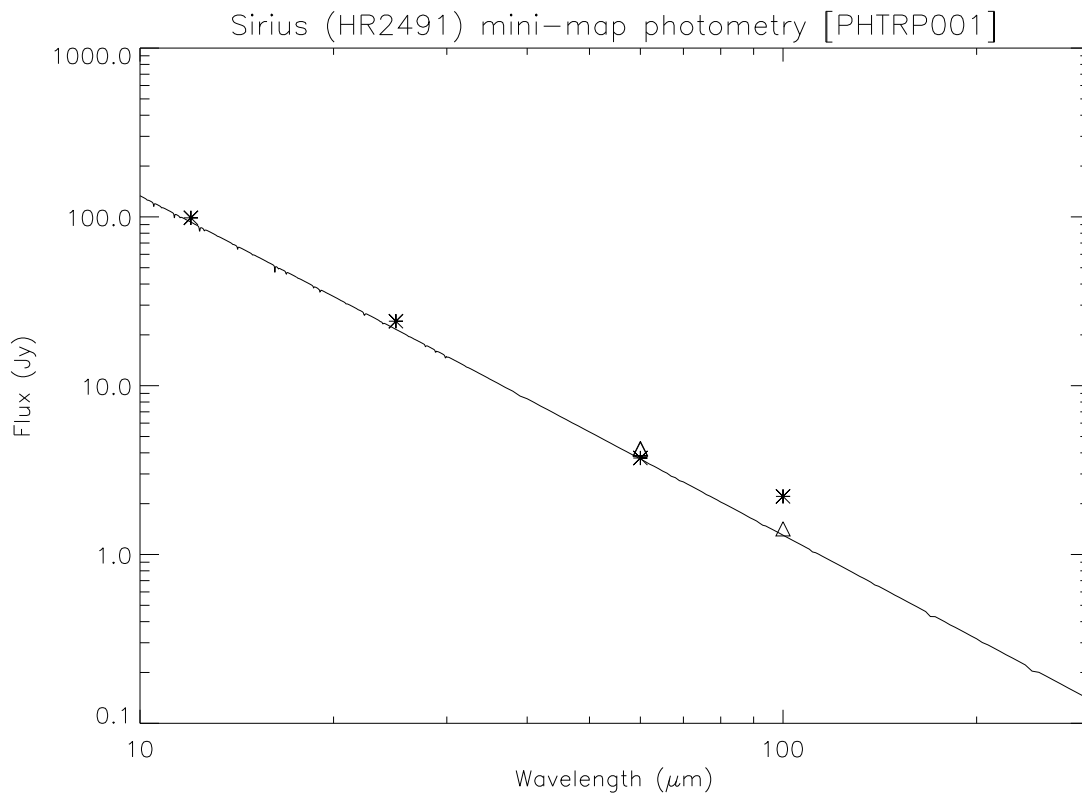
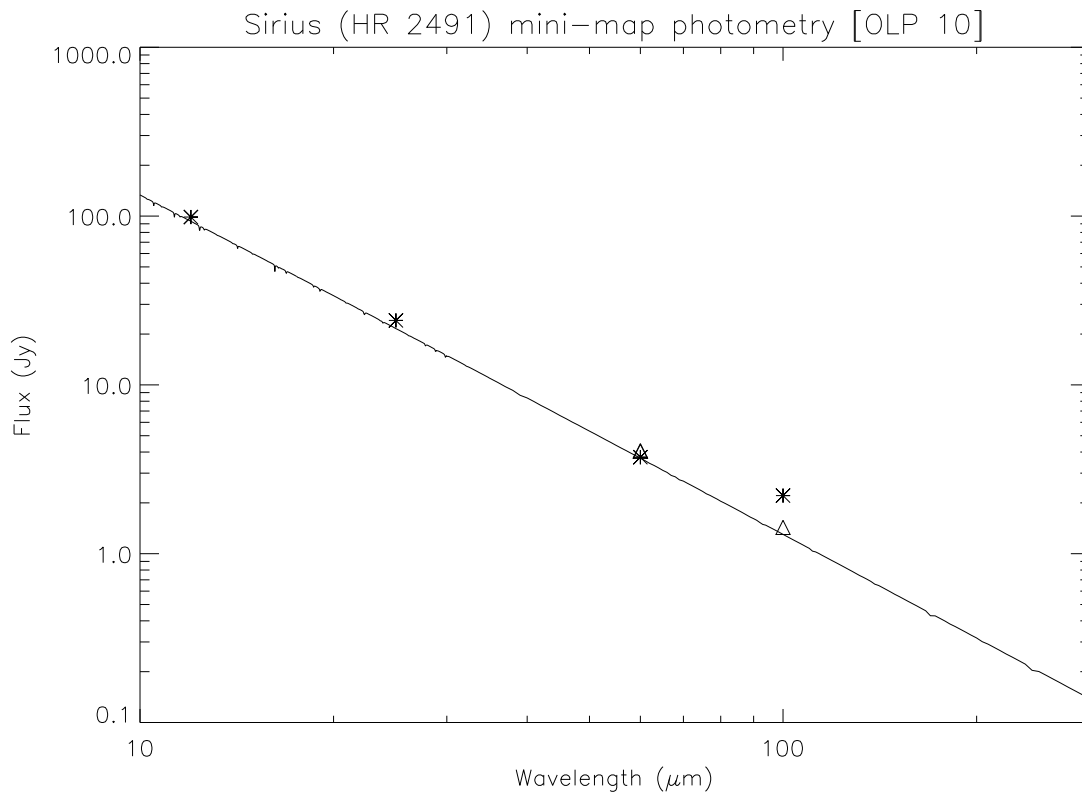


Figure 4: Comparison of PHT-C mini-map photometry with the model spectrum (plus extension out to  $300 \mu\text{m}$ ) of Sirius (HR 2491) provided by M. Cohen and with IRAS photometry for OLP 10 (upper panel) and OLP PHTRP001 (lower panel). All photometric points are color corrected for a  $10000\text{K}$  BB. The meaning of the symbols is the following: solid line: model, asterisk: IRAS, triangle: PHT-C100 (P22 AOT).

#### 4.4.5 Evaluation Log

1) point source photometry of Sirius (HR 2491) from mini-maps

Measurements:

PHT-C100:       pcas70705603 (P22 minimap)   FCS = 60  $\mu$ m  
                   pcas70705604 (P22 minimap)   FCS = 100  $\mu$ m  
                   pcas72301711 (P22 minimap)   FCS = 60  $\mu$ m (b)

Colour correction: black body, T = 10000 K

Model:           Cohen

The PHTRP001 flux densities are those given by the SOURCEn keywords in the PGAI product headers for the above TDTs.

Det	cwl ( $\mu$ m)	OLP 10	PHTRP001	IRAS	Model	$\Delta$ (OLP 10)	$\Delta$ (PHTRP001)
C1	60.0	4.041	4.206	3.728	3.680	9.81	14.29
C1b	60.0	4.076	4.248	3.728	3.680	10.79	15.44
C1	100.0	1.431	1.418	2.208	1.302	9.88	8.93

The following table gives a comparison between the bi-weight mean and median flux densities (in Jy from the SOURCEn and SRCMEDn keywords respectively) and the bi-weight mean and median backgrounds (in Jy/pixel from the BACKFn and BFMEDn keywords respectively). No colour corrections have been applied to the flux densities in the table.

Det	cwl ( $\mu$ m)	Source Flux(Jy)		Background(Jy/pixel)	
		Bi-weight	Median	Bi-weight	Median
C1	60.0	4.307	4.222	0.709	0.688
C1b	60.0	4.458	4.344	0.848	0.852
C1	100.0	1.533	1.611	1.253	1.221

## 4.5 Point Source Photometry from PHT22 Mini-Maps: The $180\ \mu\text{m}$ flux of $\alpha$ Ari (HR 617)

### 4.5.1 Motivation

HR 617 ( $\alpha$  Ari) is one of the brightest calibration stars. There exists a mini-map in the C200  $180\ \mu\text{m}$  filter which can be used to check out the pipeline algorithm for this filter.

### 4.5.2 Method

We compare the background subtracted, color corrected flux values of OLP V10 and OLP PHTRP001 results against the model prediction.

### 4.5.3 Results

The comparison of OLP 10 and OLP PHTRP001 photometry with the model is given in part 1 of the evaluation log. Fig. 5 displays the photometric results extracted from the mini-map PCAS product for OLP V10 (top) and the PGAI header for PHTRP001 (bottom). The C200 photometry at a flux level of 250 mJy is as good as 30 %. The IRAS  $100\ \mu\text{m}$  FSC flux is only an upper limit.

### 4.5.4 Conclusions

- This test case shows that the good absolute photometric accuracy found for the PHTRP001 mini-map processing holds for C200 filters down to 0.25 Jy with an accuracy of 15 %, which is an improvement on the PCAS processed product of 30 %

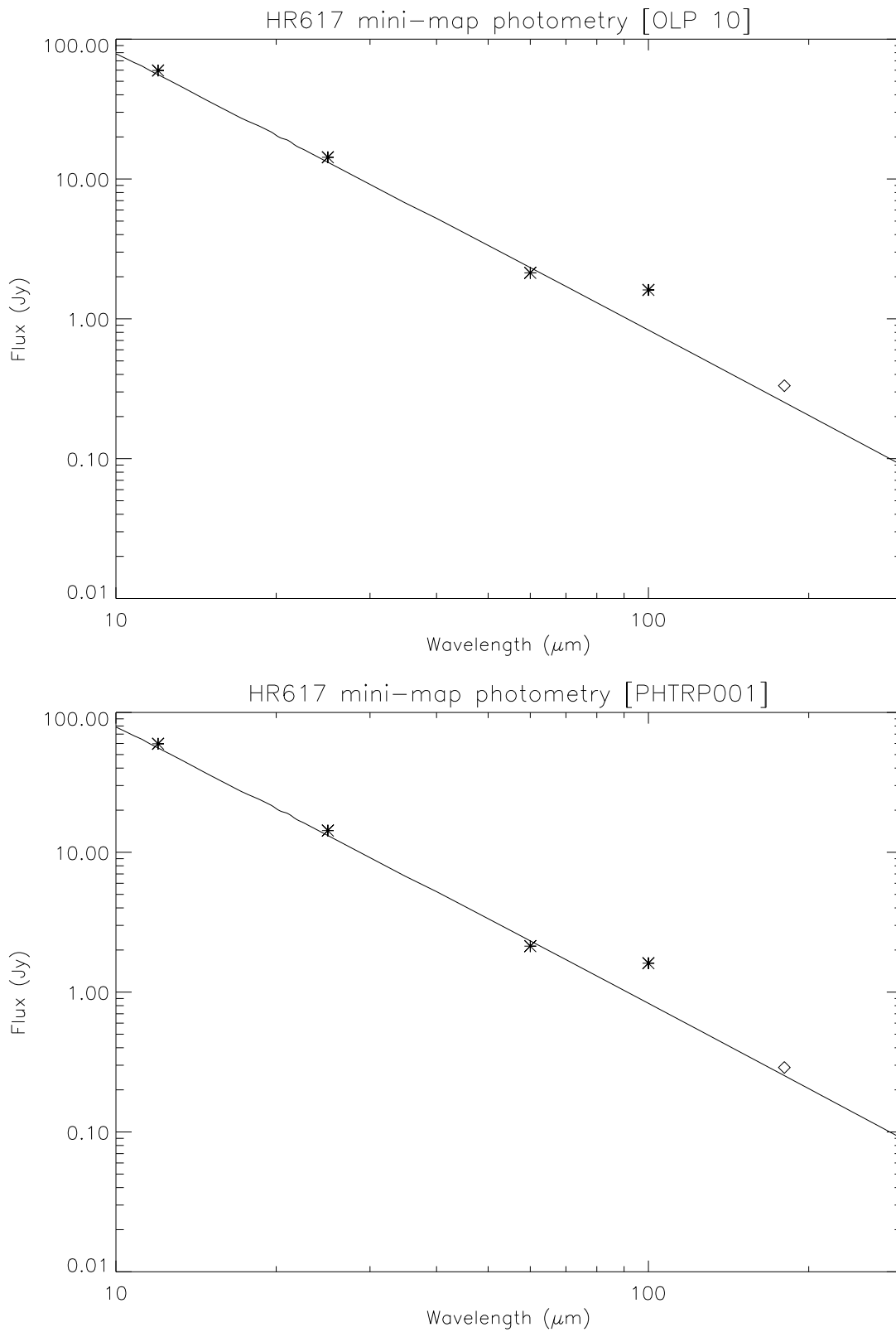


Figure 5: Comparison of PHT-C mini-map photometry with the model spectrum (plus extension out to 300  $\mu\text{m}$ ) of HR 617 provided by M. Cohen and with IRAS photometry for OLP 10 (upper panel) and OLP PHTRP001 (lower panel). All photometric points are color corrected for a 4000 K BB. The meaning of the symbols is the following: solid line: model, asterisk: IRAS, diamond: PHT-C200 (P22 AOT).

### 4.5.5 Evaluation Log

1) point source photometry of HR 617 from mini-maps

Measurements:

PHT-C200: pcas79001902 (P22 minimap) FCS = 180 um

Colour correction: black body, T = 4000 K

Model: Cohen

The PHTRP001 flux densities are those given by the SOURCE1 keyword in the PGAI product header for the above TDTs.

Det	cwl ( $\mu\text{m}$ )	OLP 10	PHTRP001	IRAS	Model	$\Delta$ (OLP 10)	$\Delta$ (PHTRP001)
C2	180.0	0.333	0.289		0.253	31.59	14.31

The following table gives a comparison between the bi-weight mean and median flux densities (in Jy from the SOURCE1 and SRCMED1 keywords respectively) and the bi-weight mean and median backgrounds (in Jy/pixel from the BACKF1 and BFMED1 keywords respectively). No colour corrections have been applied to the flux densities in the table.

Det	cwl ( $\mu\text{m}$ )	Source Flux(Jy)		Background(Jy/pixel)	
		Bi-weight	Median	Bi-weight	Median
C2	180.0	0.318	0.315	2.797	2.771

## 4.6 Point Source Photometry from PHT22 Mini-Maps: The $90\ \mu\text{m}$ flux of HR 6464

### 4.6.1 Motivation

HR 6464 is a faint calibration star in the C100 range. There exists a mini-map in the C100  $90\ \mu\text{m}$  filter which can be used to check out the pipeline algorithm for a faint source in this filter.

### 4.6.2 Method

We compare the background subtracted, color corrected flux values of OLP V10 and OLP PHTRP001 results against the model prediction.

### 4.6.3 Results

The comparison of OLP 10 and OLP PHTRP001 photometry with the model is given in part 1 of the evaluation log. Fig. 6 displays the photometric results extracted from the mini-map PCAS product (top) and the PGAI header for the PHTRP001 processing (bottom). An absolute photometric accuracy of 30% is achieved for a source flux close to 100 mJy. The IRAS  $100\ \mu\text{m}$  FSC flux has only medium quality.

### 4.6.4 Conclusions

- This test case shows that the good absolute photometric accuracy holds for the PHTRP001 processing for C100 filters down to 0.12 Jy with an accuracy of 30%.

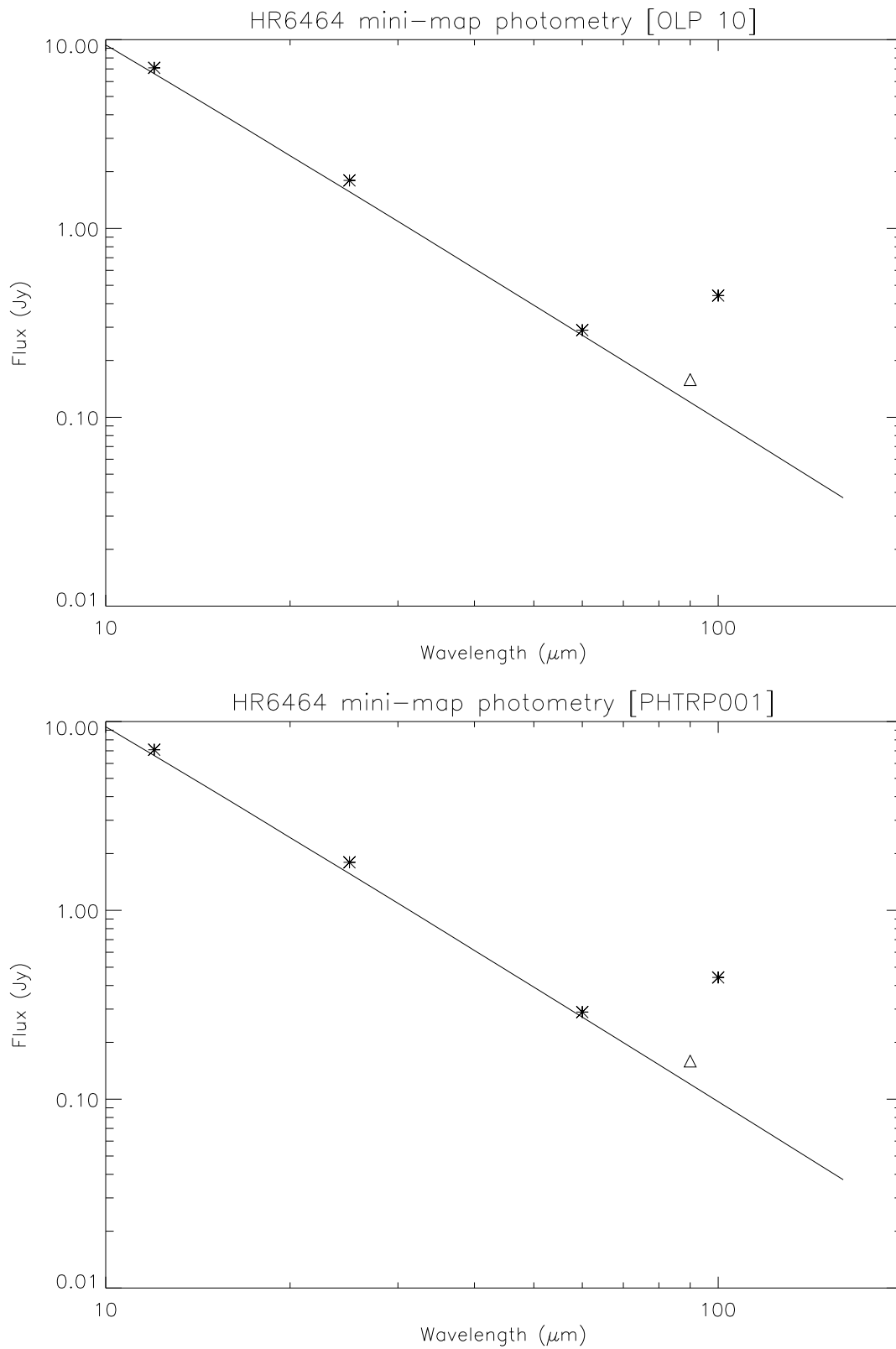


Figure 6: Comparison of PHT-C mini-map photometry with the model spectrum of HR 6464 provided by P. Hammersley and with IRAS photometry for OLP 10 (upper panel) and OLP PHTRP001 (lower panel). All photometric points are color corrected for a 3893K BB. The meaning of the symbols is the following: solid line: model, asterisk: IRAS, triangle: PHT-C100 (P22 AOT).

#### 4.6.5 Evaluation Log

1) point source photometry of HR 6464 from mini-maps

Measurements:

PHT-C100:           pcas78300465 (P22 minimap)    FCS = 90  $\mu$ m

Colour correction: black body, T = 3893K

Model:               Hammersley

The PHTRP001 flux density is that given by the SOURCE1 keyword in the PGAI product header for the above TDT.

Det	cwl ( $\mu$ m)	OLP 10	PHTRP001	IRAS	Model	$\Delta$ (OLP 10)	$\Delta$ (PHTRP001)
C1	90.0	0.158	0.159		0.120	31.88	32.52

The following table gives a comparison between the bi-weight mean and median flux densities (in Jy from the SOURCE1 and SRCMED1 keywords respectively) and the bi-weight mean and median backgrounds (in Jy/pixel from the BACKF1 and BFMED1 keywords respectively). No colour corrections have been applied to the flux densities in the table.

Det	cwl ( $\mu$ m)	Source Flux(Jy)		Background(Jy/pixel)	
		Bi-weight	Median	Bi-weight	Median
C1	90.0	0.185	0.178	0.359	0.353



## 4.7 Point Source Photometry from PHT22 Mini-Maps: The 60 $\mu\text{m}$ flux of HD 185144

### 4.7.1 Motivation

HD 185144 is a faint calibration star in the C100 range. There exists a mini-map in the C100 60  $\mu\text{m}$  filter which can be used to check out the pipeline algorithm for a faint source in this filter.

### 4.7.2 Method

We compare the background subtracted, color corrected flux values of OLP V10 and OLP PHTRP001 results against the scaled model predictions by Hammersley and IRAS photometry.

### 4.7.3 Results

The comparison of OLP 10 and OLP PHTRP001 photometry with the model is given in part 1 of the evaluation log. Fig. 7 displays the photometric results extracted from the mini-map PCAS product for OLP V10 (top) and the PGAI header for OLP PHTRP001 (bottom). The C100 photometry is accurate as 20 % for this low flux level of less than 100 mJy. The IRAS 60 and 100  $\mu\text{m}$  FSC fluxes are only upper limits.

### 4.7.4 Conclusions

- This test case verifies the good absolute photometric accuracy found for PCAS products and gives for the C100 60  $\mu\text{m}$  filter an accuracy of better than 15 % for an expected flux level of 100 mJy.

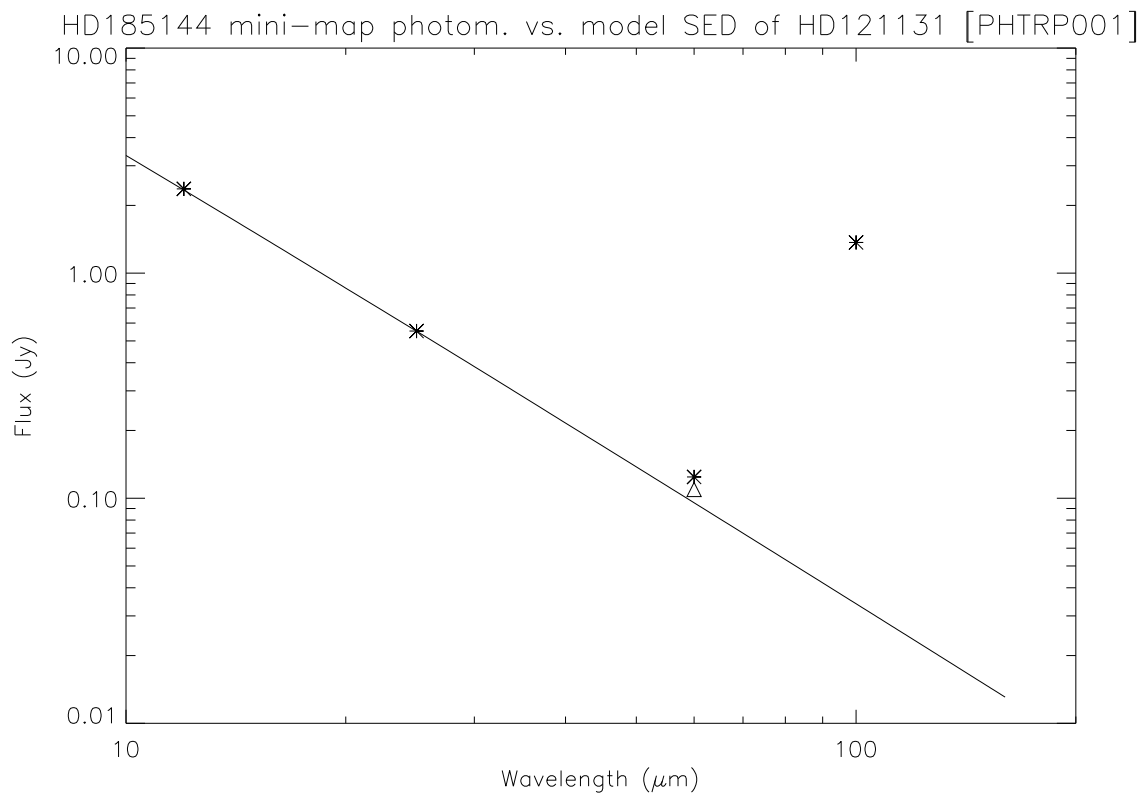
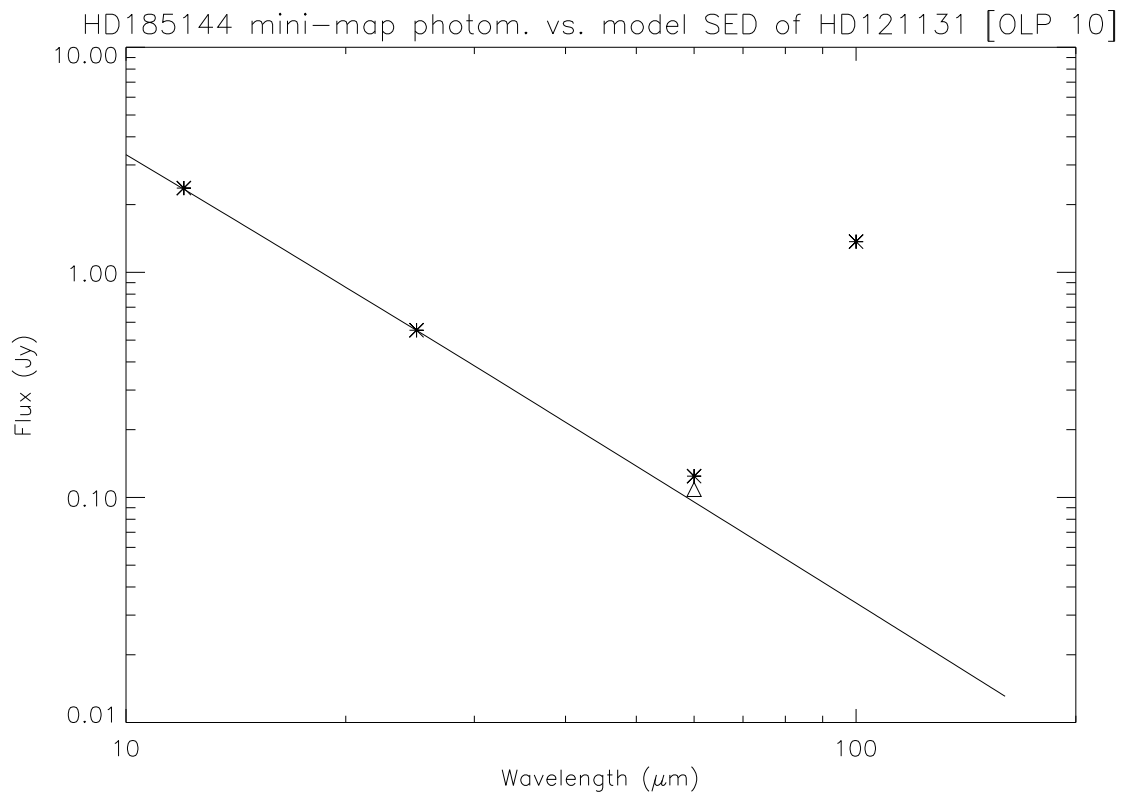


Figure 7: Comparison of PHT-C mini-map photometry of HD 185144 (K0V,  $m_v = 4.70$  mag) with the scaled model of HD 121131 (K1V,  $m_v = 8.34$  mag) provided by P. Hammersley and with IRAS photometry for OLP 10 (upper panel) and OLP PHTRP001 (lower panel). All photometric points are color corrected for a 5103K BB. The meaning of the symbols is the following: solid line: model, asterisk: IRAS, triangle: PHT-C200 (P22 AOT).

#### 4.7.5 Evaluation Log

1) point source photometry of HD 185144 from mini-maps versus scaled HD121131 model.

Measurements:

PHT-C100:           pcas69500449 (P22 minimap)    FCS = 60  $\mu$ m

Colour correction: black body, T = 5103K

Model:               Hammersley (HD121131) scaled with V-mag 4.70mag(star)/8.34mag(ref)

The PHTRP001 flux density is that given by the SOURCE1 keyword in the PGAI product header for the above TDTs.

Det	cwl ( $\mu$ m)	OLP 10	PHTRP001	IRAS	Model	$\Delta$ (OLP 10)	$\Delta$ (PHTRP001)
C1	60.0	0.109	0.109	0.124	0.095	13.71	14.52

The following table gives a comparison between the bi-weight mean and median flux densities (in Jy from the SOURCE1 and SRCMED1 keywords respectively) and the bi-weight mean and median backgrounds (in Jy/pixel from the BACKF1 and BFMED1 keywords respectively). No colour corrections have been applied to the flux densities in the table.

Det	cwl ( $\mu$ m)	Source Flux(Jy)		Background(Jy/pixel)	
		Bi-weight	Median	Bi-weight	Median
C1	60.0	0.116	0.099	0.426	0.425

## 4.8 Point Source Photometry from PHT22 Mini-Maps: The FIR SED of Vega (HR 7001)

### 4.8.1 Motivation

Vega is one of the two primary calibrators. However, in the FIR it shows an excess due to a cool disk component, which is extended. This allows the effect of source extension on the photometry from the automatic pipeline processing to be assessed.

### 4.8.2 Method

We compare the background subtracted, color corrected  $60\ \mu\text{m}$  flux value of OLP V10 and OLP PHTRP001 results against IRAS photometry and the model of a modified black body. Only the observation in the  $60\ \mu\text{m}$  filter has been processed by the PHTRP001 pipeline, since the C200 observations were executed with pixel overlap.

### 4.8.3 Results

Fig. 8 displays the photometric results extracted from the mini-map PCAS product for OLP 10 (top) and the PGAI product header for OLP PHTRP001 (bottom). For the derivation of the OLP 10  $60\ \mu\text{m}$  flux not a point source footprint but a 22 arcsec Gaussian footprint was used in order to account for the extended emission of the disk [8]. However, as the OLP PHTRP001 is processed automatically with the point source footprint, the difference between the OLP 10 and OLP PHTRP001 photometric results must be due to the different footprints used to determine the source flux density. The  $60\ \mu\text{m}$  point is relatively consistent with IRAS (within 20%), though somewhat lower (this is somewhat dependent on the source beam model). The model gives a good fit to the ISOPHOT measurements, assuming a 22 arcsec Gaussian footprint.

### 4.8.4 Conclusions

- For an extended source like Vega, the OLP PHTRP001 flux densities will be underestimates of the actual fluxes.

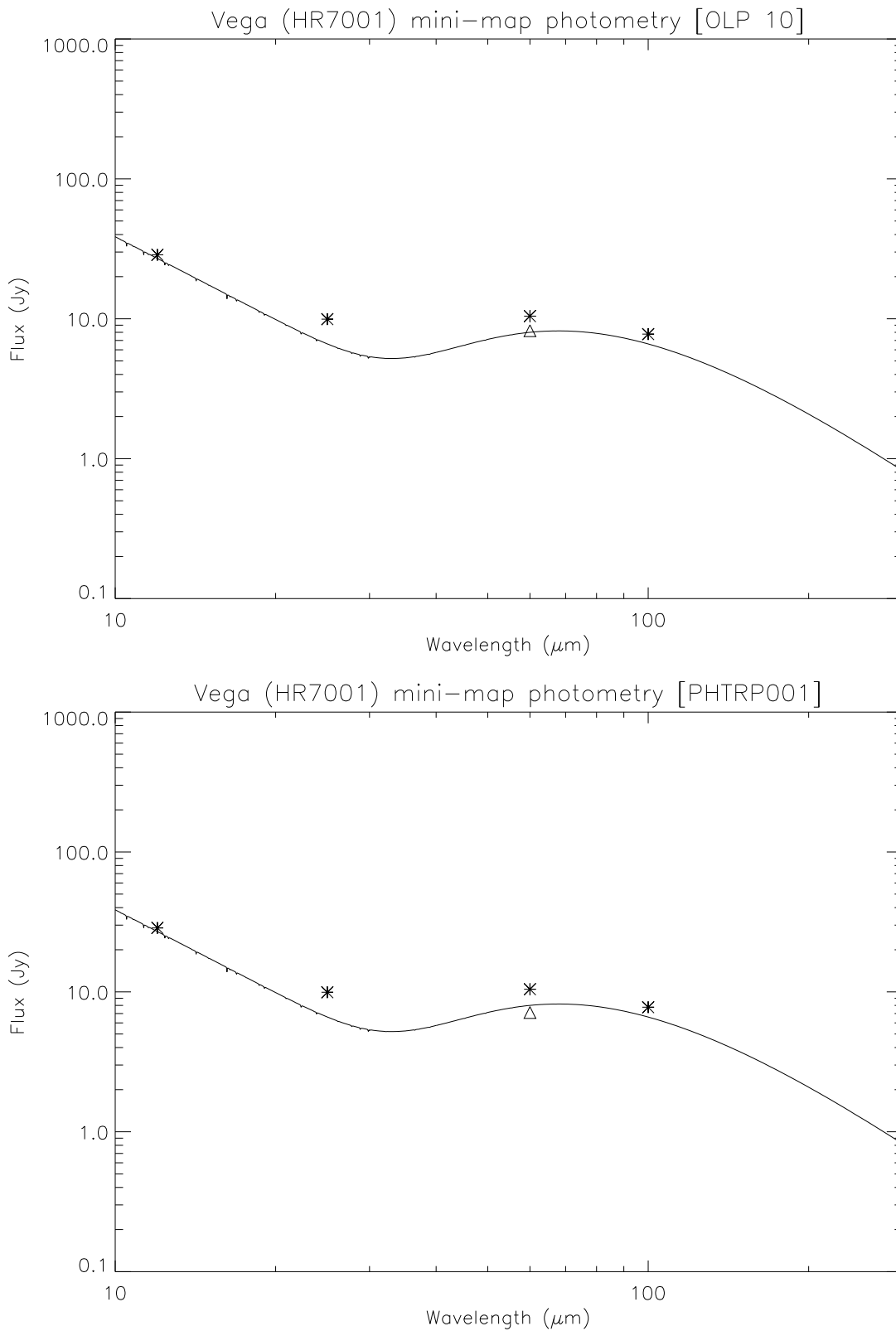


Figure 8: Comparison of PHT-C mini-map photometry with the model spectrum of Vega (HR 7001) provided by M. Cohen plus a FIR excess by a 50 K modified BB ( $\epsilon \propto \lambda^{-1}$ ) and with IRAS photometry for OLP 10 (upper panel) and OLP PHTRP001 (lower panel). The photometric points are color corrected for a 10000 K BB at  $12 \mu\text{m}$ , 2:1 mixture of 10000 K BB and 80 K modified ( $\epsilon \propto \lambda^{-1}$ ) BB at  $25 \mu\text{m}$  and 50 K modified BB for  $\lambda > 30 \mu\text{m}$ . The meaning of the symbols is the following: solid line: model, asterisk: IRAS, triangle: PHT-C100 (P22 AOT), diamond: PHT-C200 (P22 AOT).

#### 4.8.5 Evaluation Log

1) FIR photometry of Vega (HR 7001) from mini-map

Measurements:

PHT-C100:           pcas71500582 (P22 minimap)    FCS = 60  $\mu$ m

Colour correction: mod. bb, em.=1, T = 50 K

Model:               Cohen & FIR excess

The PHTRP001 flux density is that given by the SOURCE1 keyword in the PGAI product header for the above TDT.

Det	cwl ( $\mu$ m)	OLP 10	PHTRP001	IRAS	Model	$\Delta$ (OLP 10)	$\Delta$ (PHTRP001)
C1	60.0	8.216	7.119	10.445	8.004	2.64	-11.06

The following table gives a comparison between the bi-weight mean and median flux densities (in Jy from the SOURCE1 and SRCMED1 keywords respectively) and the bi-weight mean and median backgrounds (in Jy/pixel from the BACKF1 and BFMED1 keywords respectively). No colour corrections have been applied to the flux densities in the table.

Det	cwl ( $\mu$ m)	Source Flux(Jy)		Background(Jy/pixel)	
		Bi-weight	Median	Bi-weight	Median
C1	60.0	6.551	6.589	0.665	0.658

## 4.9 Point Source Photometry from PHT22 Mini-Maps: The FIR SED of HD 216956 (Formalhaut)

### 4.9.1 Motivation

HD 216956 (Formalhaut) is a FIR excess star.

### 4.9.2 Method

We compare the background subtracted, color corrected flux values of OLP V10 and OLP PHTRP001 results against IRAS photometry and the model of a modified black body with the parameters given in [9].

### 4.9.3 Results

The comparison of OLP 10 and OLP PHTRP001 photometry with the model is given in part 1 of the evaluation log. For OLP 10, fluxes have been derived assuming both a point source footprint (showing good agreement with PHTRP001) and a 22 arcsec Gaussian footprint (C1e). Assuming a similar extension of the Formalhaut disk as for Vega (cf. 4.8) increases the  $60\ \mu\text{m}$  flux by about 1.4 Jy and makes it more consistent with IRAS photometry.

### 4.9.4 Conclusions

- Assuming a point source model, the flux densities for OLP 10 and OLP PHTRP001 are in good agreement.
- This test case of an IR excess star shows how the PHTRP001 flux density can be affected if the source is extended. The derived ISOPHOT flux depends somewhat on the assumed source extension, a point source model provides a lowerflux limit.

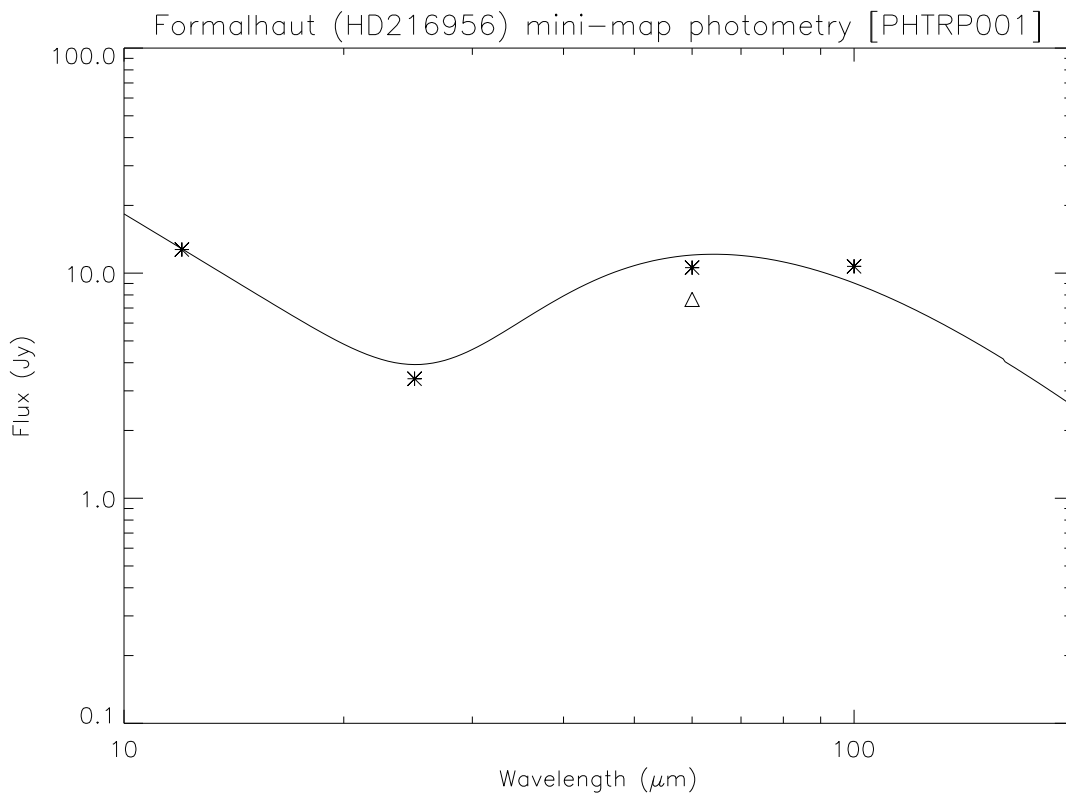
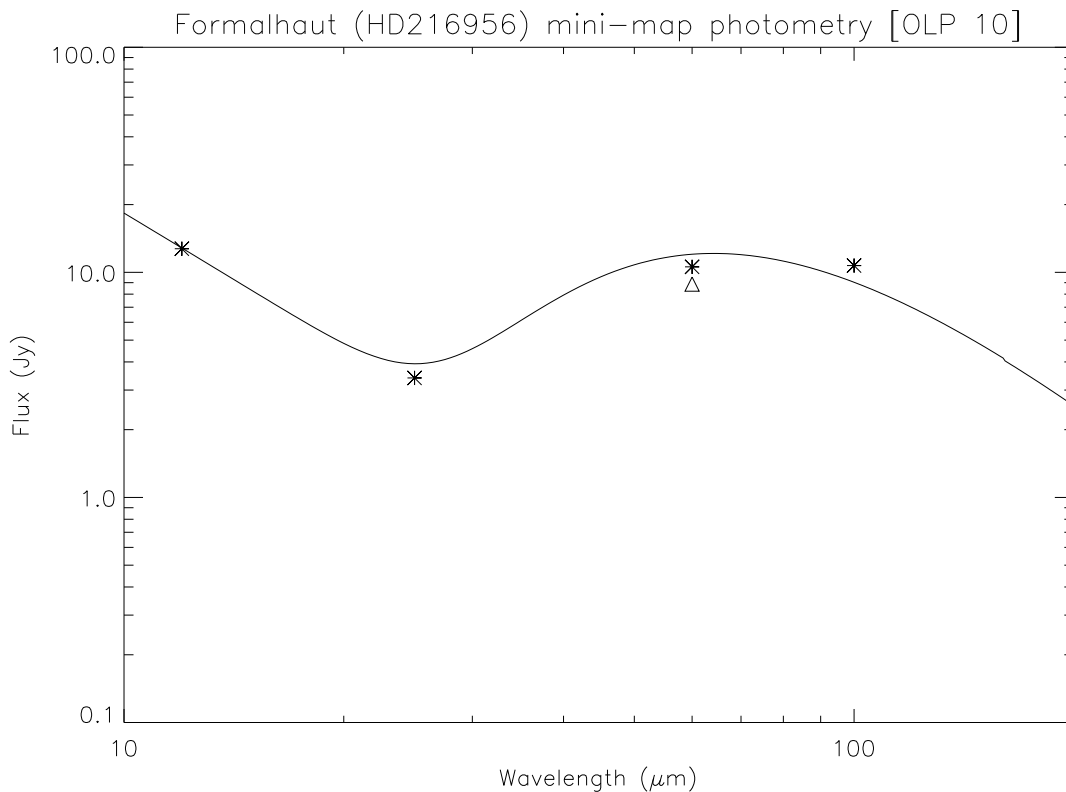


Figure 9: Comparison of PHT-C mini-map photometry of HD216956 (Formalhaut) with the scaled model spectrum of HD 158485 (HR 6514) provided by P. Hammersley plus a FIR excess by a 55 K modified BB ( $\epsilon \propto \lambda^{-1}$ ) and with IRAS photometry for OLP 10 (upper panel) and OLP PHTRP001 (lower panel). A point source footprint was assumed in reconstructing the flux from the raster map. The photometric data points are corrected for a 8390 K BB for  $\lambda < 30 \mu\text{m}$  and for a 50 K modified BB for  $\lambda > 30 \mu\text{m}$ . The meaning of the symbols is the following: solid line: model, asterisk: IRAS, triangle: PHT-C100 (P22 AOT).



#### 4.9.5 Evaluation Log

1) FIR photometry of HD 216956 (Formalhaut) from mini-map

Measurements:

PHT-C100: pcas71800269 (P22 minimap) FCS = 60  $\mu\text{m}$

Flux reconstruction: point source and  $22''$  Gaussian footprint (C1e)

Colour correction: mod. bb, em.=1, T = 50 K

Model: Hammersley & 55 K modified ( $\epsilon \propto \lambda^{-1}$ ) BB

The PHTRP001 flux density is that given by the SOURCE1 keyword in the PGAI product header for the above TDT.

Det	cwl ( $\mu\text{m}$ )	OLP 10	PHTRP001	IRAS	Model	$\Delta$ (OLP 10)	$\Delta$ (PHTRP001)
C1	60.0	7.449	7.643	10.576	12.035	-38.10	-36.49
C1e	60.0	8.866	-	10.576	12.035	-26.33	-

The following table gives a comparison between the bi-weight mean and median flux densities (in Jy from the SOURCE1 and SRCMED1 keywords respectively) and the bi-weight mean and median backgrounds (in Jy/pixel from the BACKF1 and BFMED1 keywords respectively). No colour corrections have been applied to the flux densities in the table.

Det	cwl ( $\mu\text{m}$ )	Source Flux(Jy)		Background(Jy/pixel)	
		Bi-weight	Median	Bi-weight	Median
C1	60.0	7.033	7.023	0.891	0.909

## 4.10 Point Source Photometry from PHT22 Mini-Maps: The SED of the Quasar PG 1700+518

### 4.10.1 Motivation

This is another example of a faint source observed in the 60 and 100  $\mu\text{m}$  filters.

### 4.10.2 Method

We compare the background subtracted flux of OLP V10 and OLP PHTRP001 results against IRAS photometry. The IRAS 100  $\mu\text{m}$  FSC flux is an upper limit at around 1 Jy.

### 4.10.3 Results

The comparison of OLP 10 and OLP PHTRP001 photometry with IRAS is given in part 1 of the evaluation log. Fig. 10 displays the photometric results extracted from the mini-map PCAS product for OLP 10 (top) and the PGAI header for PHTRP001 (bottom). The consistency with IRAS 60  $\mu\text{m}$  photometry is very good.

### 4.10.4 Conclusions

- A good consistency of 60  $\mu\text{m}$  mini-map photometry with IRAS is found.
- The mini-map technique allows good photometric results at wavelengths beyond 60  $\mu\text{m}$  considerably deeper than IRAS FSC.

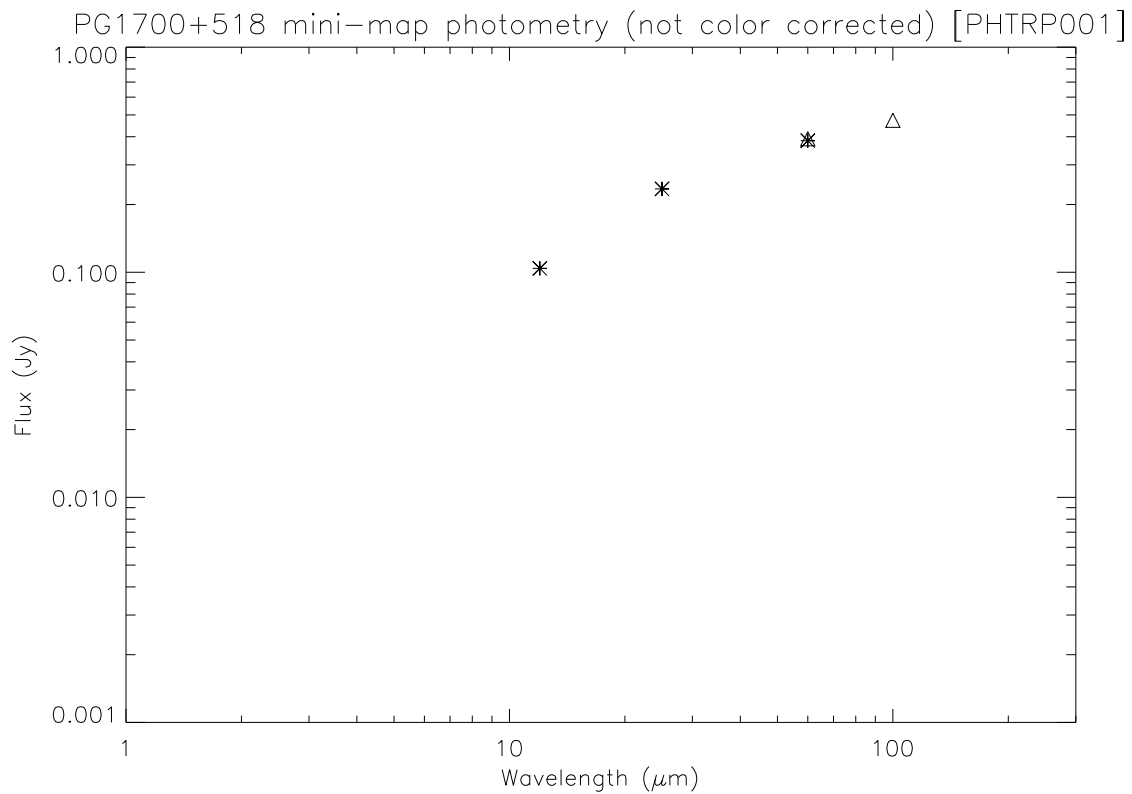
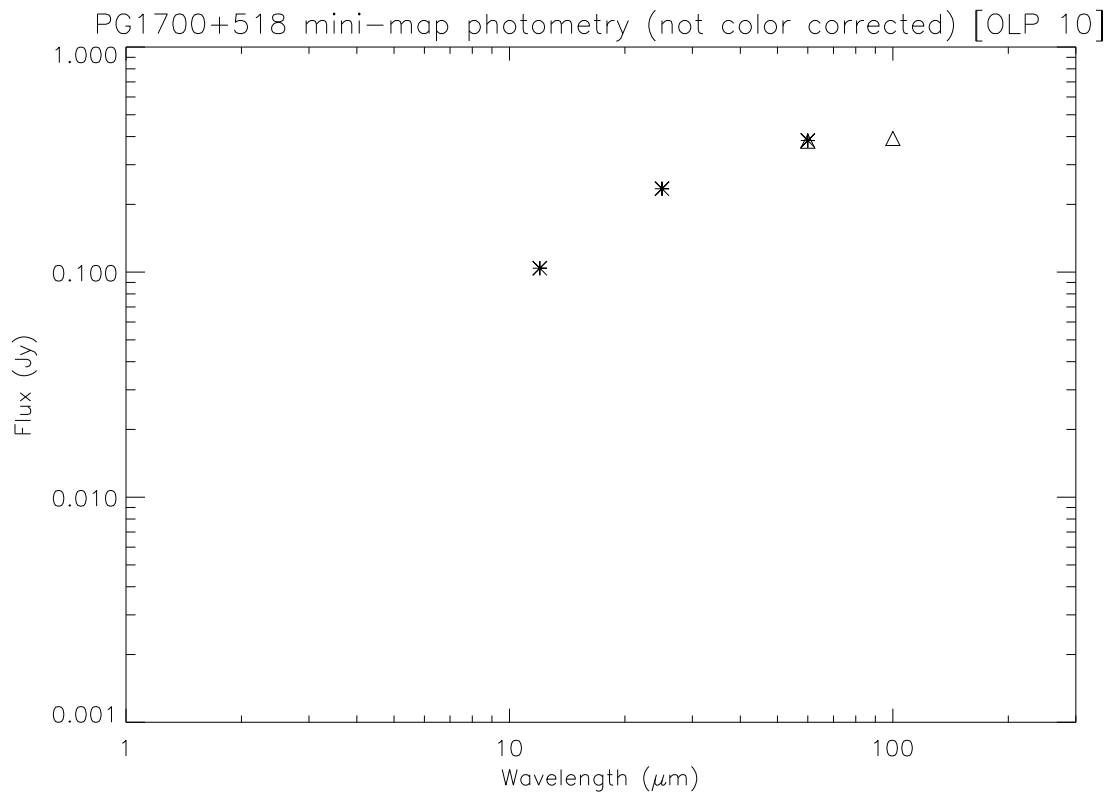


Figure 10: Comparison of PHT-C mini-map photometry of PG 1700+518 with IRAS photometry for OLP 10 (upper panel) and OLP PHTRP001 (lower panel). No color correction was applied. The meaning of the symbols is the following: asterisk: IRAS, triangle: PHT-C100 (P22 AOT), diamond: PHT-C200 (P22 AOT).

#### 4.10.5 Evaluation Log

1) Photometry of PG 1700+518 from mini-map

Measurements:

PHT-C100:           pcas51800420 (P22 minimap)    FCS = 60, 100 um

The PHTRP001 flux density is that given by the SOURCEi keywords in the PGAI product header for the above TDT.

Det	cwl ( $\mu\text{m}$ )	OLP 10	PHTRP001	IRAS
C1	60.0	0.382	0.392	0.384
C1	100.0	0.393	0.473	

The following table gives a comparison between the bi-weight mean and median flux densities (in Jy from the SOURCEn and SRCMEDn keywords respectively) and the bi-weight mean and median backgrounds (in Jy/pixel from the BACKFn and BFMEDn keywords respectively). No colour corrections have been applied to the flux densities in the table.

Det	cwl ( $\mu\text{m}$ )	Source Flux(Jy)		Background(Jy/pixel)	
		Bi-weight	Median	Bi-weight	Median
C1	60.0	0.473	0.470	0.427	0.401
C1	100.0	0.392	0.377	0.355	0.345

## 5 Summary and Conclusions

- Raster mode mini-map processing in the PHT pipeline PHTRP001 has been successfully validated.
- The OLP V10 Calibration accuracies have been confirmed for the PHTRP001 mini-map processing.
- C100 photometry gives reliable photometry ( $< 30\%$ ) down to fluxes as low as 50 mJy. However, this may depend on the cirrus confusion level, and hence the absolute surface brightness.
- C200 photometry appears to become unreliable below a flux level of 100 mJy. The absolute level may depend on the actual cirrus confusion noise of this field.
- In case of extended sources, the point source PSF factors used for flux reconstruction will result in flux densities which are lower than the actual values.

## References

- [1] U. Klaas, K. Wilke, C. Kiss, M. Radovich and P. Richards, “Report on the PHT Scientific Validation for OLP Version 9.0”, SAI/2000-014/Rp, Version 2.0, 19-December-2000.
- [2] R.J. Laureijs, U. Klaas, P.J. Richards, B. Schulz and P. Ábrahám, “The ISO Handbook, Volume V: PHT – The Imaging Photo-Polarimeter”, SAI/99-069/Dc, Version 1.2, 01-July-2001
- [3] U. Klaas and P. Richards, “Report on the PHT Scientific Validation for OLP Version 10.0”, Version 1.0, 9-April-2002.
- [4] R.J. Laureijs, “Point Spread Function Fractions Related to the ISOPHOT C100 and C200 Arrays”, IDC PHT Internal Calibration Report, Version 1.0, 29-June-1999
- [5] Cohen, M. et al. 1996, AJ 115, 1671
- [6] Cohen, M. et al. 1998, AJ 117, 2274
- [7] P.L. Hammersley, M. Jourdain De Muizon, M.F. Kessler, P. Bouchet, R.D. Joseph, H. Habing, A. Salama, L. Metcalfe, “Infrared standards for ISO. I. A new calibration of mid infrared photometry”, A&AS 128, 207, 1998
- [8] I. Heinrichsen, H.J. Walker, and U. Klaas, “Infrared Mapping of the Dust Disc around Vega”, MNRAS 293, L78, 1998
- [9] H.J. Walker & I. Heinrichsen, “ISOPHOT Observations of Dust Disks around Main Sequence (Vega-Like) Stars”, Icarus 143, 147, 2000